Available online at www.sciencedirect.com
SCIENCE DIRECT®
Journal of Nuclear Materials 335 (2004) 108–114
journal of nuclear materials
www.elsevier.com/locate/jnucmat

The effect of grain boundary misorientation on the intergranular $M_{23}C_6$ carbide precipitation in thermally treated Alloy 690

Yun Soo Lim *, Joung Soo Kim, Hong Pyo Kim, Hai Dong Cho

Nuclear Materials Technology & Development Division, Korea Atomic Energy Research Institute, P.O. Box 105, Yusong, Taejon 305-600, Republic of Korea

Received 5 April 2004; accepted 8 July 2004

Abstract

The precipitation characteristics of chromium carbides on various types of grain boundaries in Alloy 690 thermally treated at 720 °C for 10 h were studied through transmission electron microscopy. Precipitation of the intergranular chromium carbides, identified as Cr-rich $M_{23}C_6$, was retarded on the low angle grain boundaries, compared to that on the random high angle grain boundaries on which coarse and discrete ones were found. They were rarely found on the coherent twin boundaries, however, needle-like ones were evolved on the incoherent twin and twin related $\Sigma 9$ boundaries. Precipitation of the chromium carbides was also suppressed on the nearly exact coincidence site lattice boundaries such as $\Sigma 11$ and $\Sigma 15$, for which the Brandon criterion was fulfilled. The results of the intergranular $M_{23}C_6$ carbide precipitation were explained in terms of the influence of the grain boundary energy.

1. Introduction

Recently, nickel-base Alloy 690 (Ni–30wt%Cr–10wt%Fe) has become a replacement material for Alloy 600 (Ni–16wt%Cr–8wt%Fe) as steam generator tubes in nuclear power plants. Alloy 600 is well known to be very susceptible to intergranular stress corrosion cracking (IGSCC) under plant operating conditions [1]. Alloy 690, however, has been found to be immune to IGSCC in various environments [2,3]. Although no clear explanation exists for the improved IGSCC resistance in caustic and de-aerated neutral solutions, it is generally accepted that the precipitation of a high density of intergranular chromium carbides by thermal treatments improves the IGSCC resistance in primary water [4,5] and certain caustic environments [5,6]. Bruemmer et al. [7,8] suggested that the intergranular carbides promote crack tip blunting, decrease the crack tip stress state, and therefore, increase the resistance to cracking.

Precipitation of second phases, such as chromium carbides, at a grain boundary is known to occur selectively. Previous studies of steels [9–13] showed that the

* Corresponding author. Tel.: +82 042 868 2341; fax: +82 042 868 8346.
E-mail address: yslim@kaeri.re.kr (Y.S. Lim).

0022-3115/$ - see front matter © 2004 Elsevier B.V. All rights reserved.
doi:10.1016/j.jnucmat.2004.07.038

precipitation of chromium carbides is strongly influenced by the grain boundary character. Singhal and Martin [10] showed that the distribution of $M_{23}C_6$ precipitates in austenitic stainless steels is quite sensitive to the degree of grain boundary misorientation. Trillo and Murr [12,13] found that, as the annealing time of 304 stainless steels increases, $M_{23}C_6$ carbides start being precipitated on the grain boundary with a smaller grain boundary misorientation. Liu et al. [14] characterized the distribution in grain boundary character of Ni–18wt%Cr–18wt%Fe alloy with the coincidence site lattice (CSL) model, and found that the chromium carbides on the low angle grain boundary ($\Sigma 1$) and the twin related grain boundaries such as $\Sigma 9$ and $\Sigma 27$ tend to be smaller and closer spaced than those of the other Σ and random high angle grain boundaries. No carbides were observed on the coherent twin boundaries ($\Sigma 3_c$), however, needle-like $M_{23}C_6$ were evolved on the incoherent twin boundaries ($\Sigma 3_i$) in their studies [9,12–14]. All of these trends are believed to be related to the grain boundary energy, because grain boundaries with small Σ numbers usually have low energies corresponding to the energy cusps in the grain boundary energy curve [15].

The present work is an attempt to describe the correlation between the grain boundary character and the precipitation of the intergranular chromium carbides in thermally treated Alloy 690 utilizing transmission electron microscopy (TEM). The grain boundaries were characterized according to the CSL theory [16–18], and the grain boundary types were classified into low angle, special, and random high angle (or general) grain boundaries, due to the analyzed misorientation relationships. The effects of the grain boundary character on the size, density and spatial distribution of the intergranular carbides were then carefully examined. Finally, the precipitation behavior of the chromium carbides on the various grain boundary types was explained in terms of the grain boundary energy.

2. Experimental procedures

2.1. Specimen preparation and microscopic examination

Alloy 690 tubing was obtained at the thermally treated condition (hereafter, Alloy 690TT), i.e., solution annealed at 1110 °C for 2 min, and then heat treated at 720 °C for 10 h for a significant growth of the intergranular chromium carbides. The heat bulk composition of the major elements is given in Table 1.

TEM specimens were prepared by cutting longitudinal strips from the tubes, grinding them to flat slabs approximately 60 μm thick, and finally electropolishing the 3 mm discs. A 7% perchloric acid + 93% methanol solution cooled to −40 °C was used and a current of approximate 50 mA was applied for jet polishing. TEM examination was carried out with a JEOL 2000 FXII (operating voltage 200 kV). Specimens for optical and SEM examination were made by chemical etching with a solution of 2% bromine + 98% methanol. JEOL 5200 (operating voltage 25 kV) was used for scanning electron microscopy (SEM).

2.2. Grain boundary characterization

The grain orientation analysis was performed by working in a convergent beam electron diffraction mode, which results in a more accurate orientation than the conventional selective area diffraction (SAD) mode. The misorientation relationship between the adjoining grains is commonly described by an angle/axis representation; the axis of the misorientation, $[UVW]$, is a direction which is common to both grains about which the first grain must be rotated by the angle of the misorientation, Θ, in order to achieve the orientation of the second. In the present study, an analytic approach by Young et al. [19] was adopted to obtain the angle/axis pair. Each misorientation was represented in the form of the smallest-angle description (or, 'disorientation' representation) of the angle/axis pair.

The angle/axis pair representation of the grain boundary misorientation is meaningful only if it can be used to determine the 'class' of a grain boundary, i.e., low angle, random high angle, or special with a CSL orientation. Therefore, the next stage in the grain boundary analysis scheme is to evaluate the deviation of a particular boundary from the nearest CSL. In this study, an analytic method [20,21] based on matrix algebra was used to experimentally determine the deviation angle ($\Delta\Theta_d$) from the exact CSL orientation, Finally, as a guide to set up a significant upper limit (i.e., maximum allowable deviation angle, $\Delta\Theta_m$) for $\Delta\Theta_d$, the Brandon formula [16] was used, following that

$$\Delta\Theta_m = 15 \cdot \Sigma^{-1/2}. \quad (1)$$

Table 1
Chemical composition of Alloy 690TT (wt%)

Ni	Cr	Fe	C	N	S	Mo	Co	Mn	Al	Cu	Ti	Nb
Bal.	29.6	10.5	0.02	0.017	0.001	0.01	0.01	0.32	0.02	0.01	0.26	Trace

3. Results and discussion

The mean linear intercept grain size excluding twins was measured to be 32 μm [22]. An optical micrograph, Fig. 1(a), reveals many annealing twins present in Alloy 690TT due to its low stacking fault energy. A twin can strongly affect the precipitation behavior of the intergranular chromium carbides, since an abrupt change of the misorientation occurs when the twin boundary impinges on a grain boundary. The intergranular chromium carbides were significantly developed by thermal treatment on most of the grain boundaries except some special boundaries such as the coherent twin boundaries (Fig. 1(b)). Fig. 2(a) is a TEM bright field image, and Fig. 2(b) is the related SAD pattern taken from the circled region in Fig. 2(a). From the diffraction pattern analysis, the intergranular chromium carbides were identified as chromium-rich (Cr-rich) $M_{23}C_6$. Cr-rich $M_{23}C_6$ has a face-centered cubic (fcc) structure, the same as Alloy 690, with a lattice constant of 1.065 nm [23], which is approximately three times larger than that of Alloy 690 of 0.3574 nm [24]. It is well known that

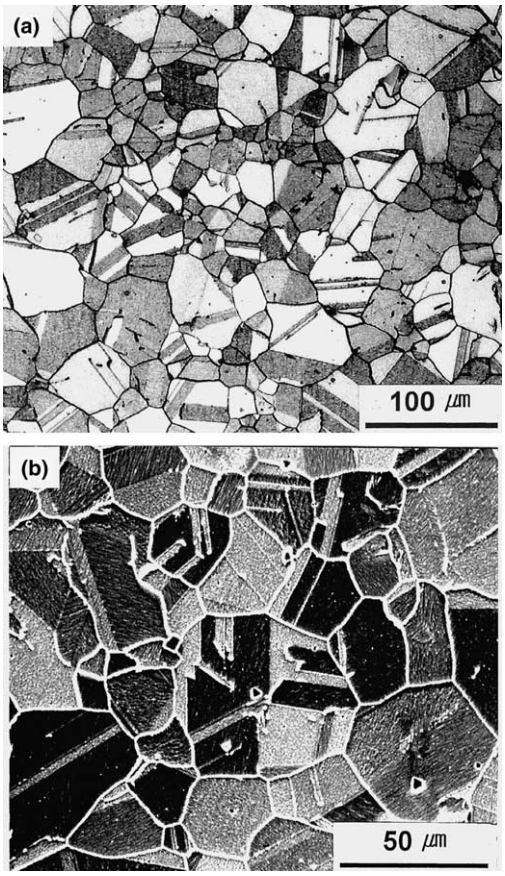

Fig. 1. (a) Optical and (b) SEM micrographs of Alloy 690TT, etched in 2% bromine + 98% methanol.

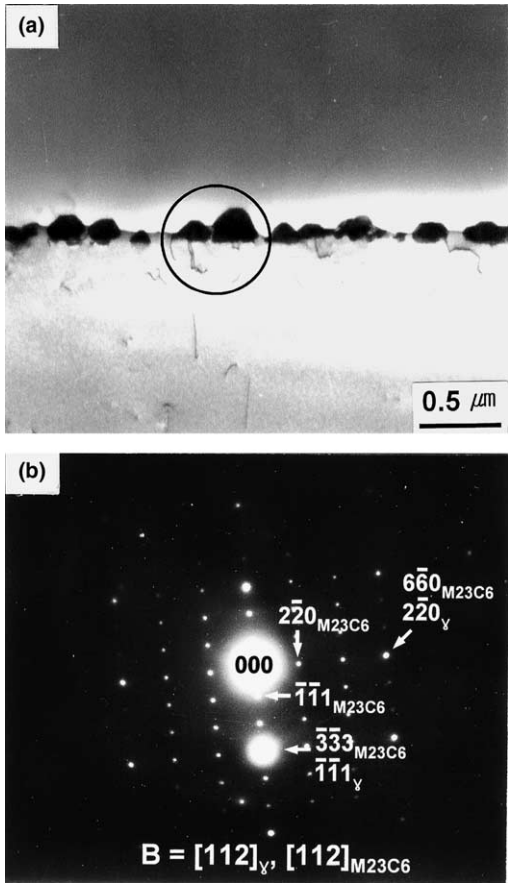

Fig. 2. (a) Grain boundary Cr-rich $M_{23}C_6$ carbides, and (b) the related SADP obtained from the circled region in (a) with B = [1 1 2].

Cr-rich $M_{23}C_6$ has a cube–cube orientation relationship such as $\{100\}_{\gamma}\|\{100\}_{M_{23}C_6}$, $\langle 100\rangle_{\gamma}\|\langle 100\rangle_{M_{23}C_6}$ with one grain, as shown in Fig. 2(b).

In the present experiment, a low angle grain boundary was defined as one having a misorientation angle less than 15° between two adjoining grains without any CSL relationship such as 12.68°/[1 0 0] of the $\Sigma 41_a$ CSL boundary. The typical intergranular carbide morphology at the low angle grain boundary is shown in Fig. 3(a), and the Kikuchi diffraction patterns from the grains in Fig. 3(a) under the same tilting condition are shown in Fig. 3(b) and (c). The $\Theta/[UVW]$ was measured as 3.5°/[1 1 1] from the analysis of the diffraction patterns. Another example of the precipitation morphology with a 5.7°/[2 0 1] low angle misorientation relationship is shown in Fig. 3(d). As seen from the figures, fine and faceted carbides were densely distributed on the boundaries, from which it is believed that the carbide morphology corresponds to the 'early stage of growth' after nucleation.

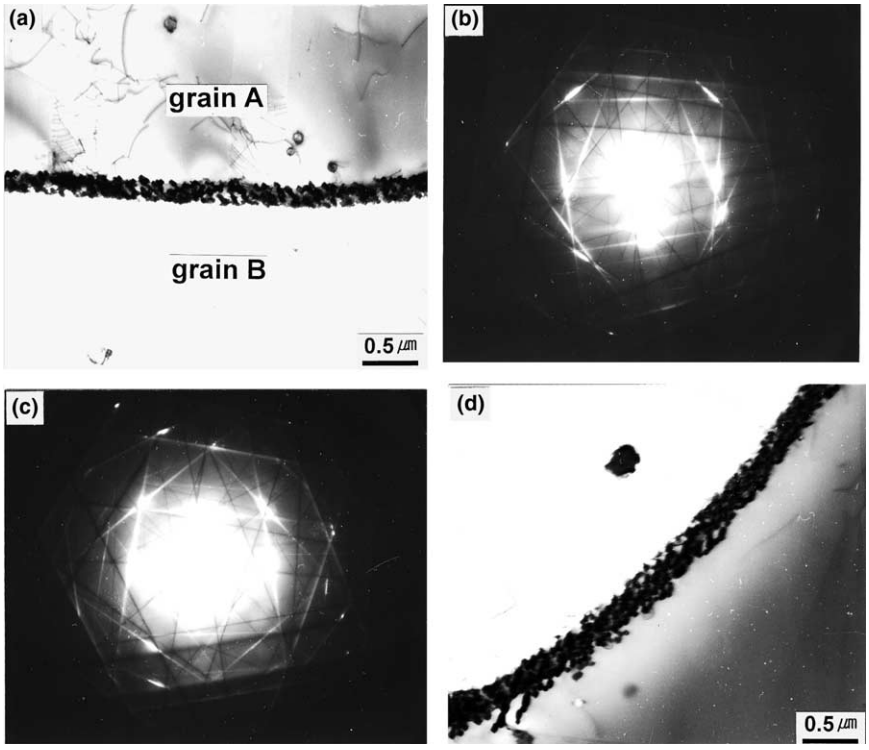

Fig. 3. (a) Low angle grain boundary with small and faceted Cr-rich $M_{23}C_6$ carbides, (b) and (c) Kikuchi diffraction patterns from grain A and grain B in (a), respectively. (d) Another example of a low angle grain boundary.

Liu et al. [14] found that the portion of random high angle grain boundaries in Ni–18wt%Cr–18wt%Fe alloy was about 80%, discounting the contributions from the $\Sigma 3$ twin boundaries and $\Sigma 3^n$ ($n = 2, 3, \ldots$) twin related boundaries. Their results were in good agreement with that predicted theoretically for a random polycrystalline aggregate [25]. The grain boundaries in Fig. 4 were interpreted as random high angle ones, because the misorientation angles were above 15° without having any precise CSL misorientations up to $\Sigma 49$ within the limit of the maximum allowable deviations given by the Brandon criterion (Eq. (1)). As shown in the figures, coarse and irregular carbides were discretely distributed on the grain boundaries, and these are the ones commonly found in thermally treated Alloy 690. In Fig. 4(a), some faceted carbides appeared to be combined with each other, to form a large irregular shape. Therefore, the time development of the precipitation of the intergranular carbides on these grain boundaries corresponds to the 'stage of concurrent coalescence and growth'. This feature is quite different, in spite of the same heat treatment conditions, from the case of the low angle grain boundary on which the tiny carbides were separately distributed. These results can be interpreted as that the nucleation rate of the carbides is high but their growth is slow on the low angle grain boundary. Therefore, it can be thought that the precipitation of the intergranular chromium carbides is retarded, even though their total volume fraction on that grain boundary seems to be as large as that on the random high angle grain boundary.

A twin and its related boundaries resulting from multiple twinning are frequent and easily found in this alloy. Most of the coherent twin boundaries ($\Sigma 3_c$) were found to have a negligible deviation from the precise $\Sigma 3$ CSL misorientation of 60°/[1 1 1], and the carbides were never found on the boundaries under the present experimental conditions, as shown in Fig. 5(a). On the other hand, needle-like carbides were precipitated on the incoherent twin boundaries ($\Sigma 3_i$), as shown in Fig. 5(b). They appeared to grow parallel to the coherent twin boundary, as reported [9,26]. It was confirmed from the SAD patterns that the carbides, Cr-rich $M_{23}C_6$, also had a cube–cube orientation relationship with the matrix, the same as in the case of the intergranular carbides. The difference in carbide precipitation on the coherent and incoherent twin boundaries demonstrates the importance of the orientation of the grain boundary plane itself, in addition to the misorientation/axis description, for the precipitation of the intergranular carbides. The coherent twin boundary is parallel to the {1 1 1} twining plane, and the atoms in the boundary

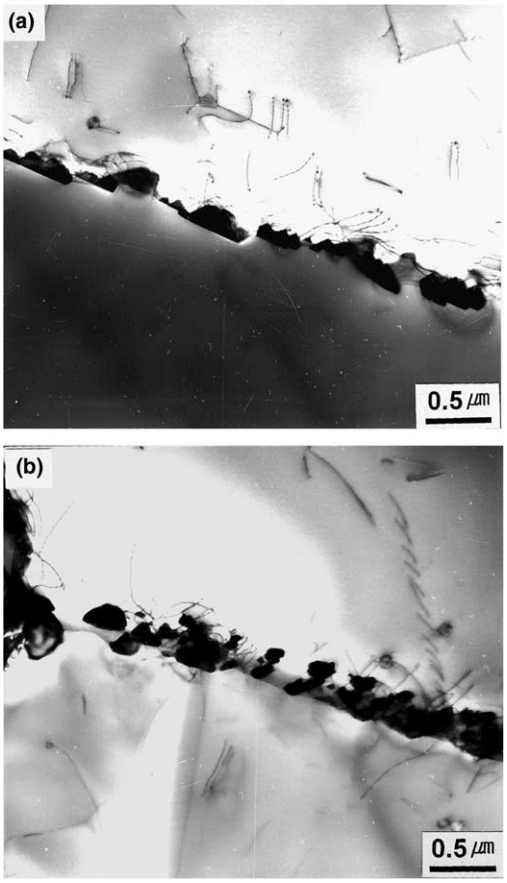

Fig. 4. Random high angle grain boundaries with coarse and discrete Cr-rich $M_{23}C_6$ on the boundaries.

fit perfectly into both grains. The atoms in the boundary are essentially in undistorted positions, resulting in an extremely low energy in comparison with the energy of a random high angle grain boundary. However, the incoherent twin boundary does not lie exactly parallel to the twining plane, and the atoms do not fit perfectly into each grain. Therefore, the boundary energy is much higher than the energy of the coherent twin boundary, even though it is still much lower than that of the random high angle grain boundary. Fig. 5(c) shows a twin related Σ9 boundary with 39.8°/[1 1 0] misorientation relationship, which was formed by an impingement of the growing twins. As shown in the figure, tiny and needle-like carbides were precipitated on that boundary and grew parallel to the coherent twin boundary, the same as in the case of the incoherent twin boundary.

Since Alloy 690 has a low stacking fault energy, most of the special boundaries consisted of twin and its related boundaries, and other Σ boundaries rarely occurred. In spite of this fact, some CSL boundaries

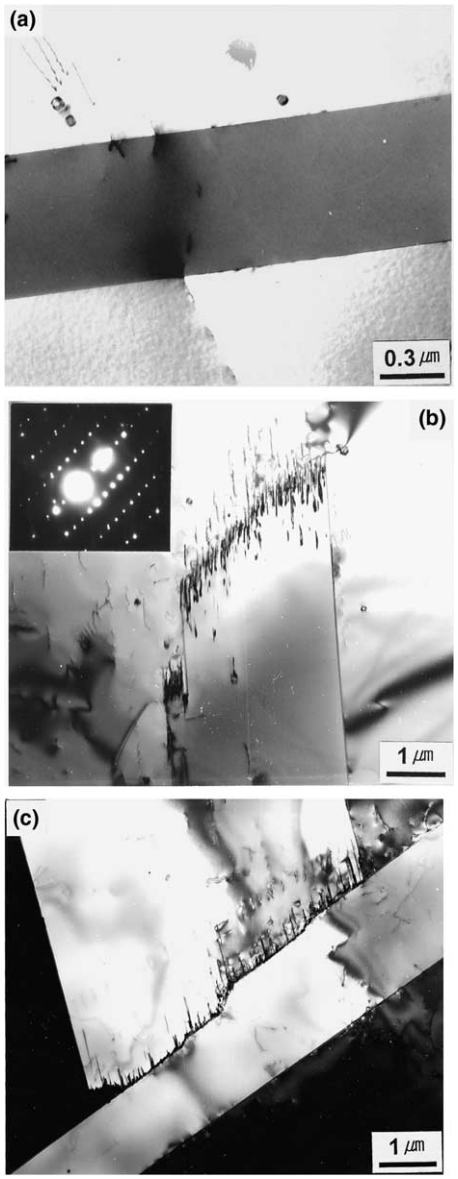

Fig. 5. (a) Coherent twin $\Sigma 3_c$, (b) incoherent twin $\Sigma 3_i$, and (c) twin related Σ9 boundaries.

were found, and Fig. 6 shows the Σ11 and Σ15 boundaries. The experimental deviations of the boundaries from the precise CSL misorientation were much smaller than the ones calculated by the Brandon formula. Therefore, they were well classified as the CSL boundaries. The carbides were not precipitated on the Σ15 boundary, and tiny ones were densely distributed on the Σ11 boundary (Fig. 6). From the above results, it can be seen that the precipitation of the intergranular carbides is suppressed on the CSL boundaries, as compared to the case of the random high angle grain boundaries.

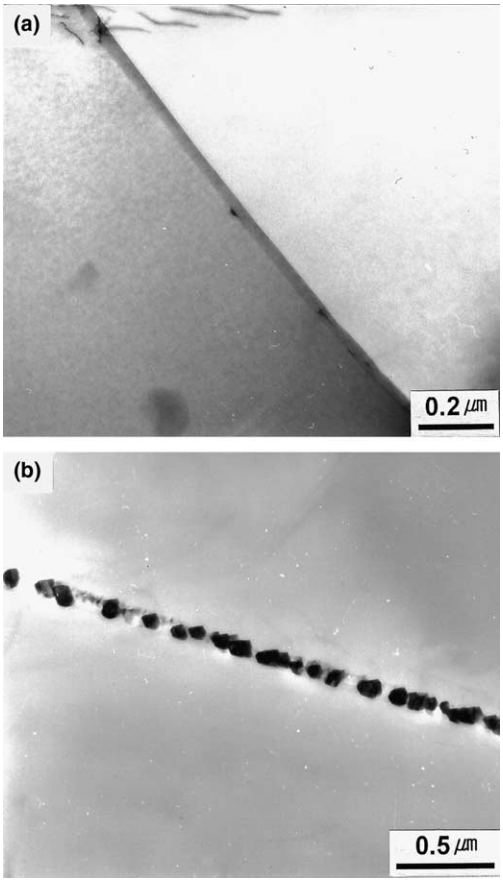

Fig. 6. Some CSL boundaries with Σ values of (a) 15 and (b) 11. The precipitation of the intergranular Cr-rich $M_{23}C_6$ was suppressed on these boundaries.

Discontinuous precipitates are commonly found in nickel-base alloys [3,26], as shown in Fig. 7. It is well known that discontinuous precipitation is associated with the concurrent grain boundary migration, and is largely dependent on the grain boundary energy, mobility and diffusivity, which depends in turn on the grain boundary structure [27]. Therefore, it is considered that discontinuous precipitation can be preferentially initiated on the grain boundaries with a particular misorientation relationship and grain boundary structure [28]. In addition, Fig. 7 illustrates how the twin boundary (denoted 'TB') influences the intergranular precipitation. The intergranular carbides were discontinuously precipitated in the cellular form on the grain boundary enclosed by the twin, however, particulate precipitates were evolved on the other part of the same grain boundary. From the above results, it can be concluded that an interception by the twins may result in large changes in the misorientation and hence in the structure of the parent boundary, from which drastic changes in the

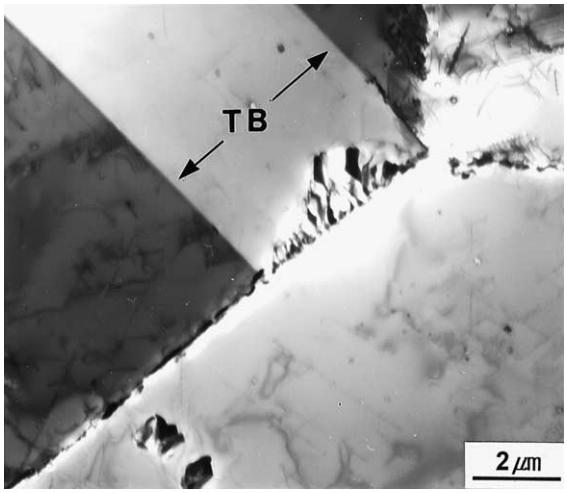

Fig. 7. Typical discontinuous precipitates of Cr-rich $M_{23}C_6$ in thermally treated Alloy 690. The twin boundaries are denoted as TB.

precipitation behavior of the intergranular carbides are expected. In the alloy, other intragranular carbides were not observed under the present heat treatment conditions.

When classifying a grain boundary using the CSL model, it is quite important to correctly estimate its deviation from a precise CSL misorientation and to determine if it comes under the category of a CSL boundary. Fixing the maximum allowable deviation from the exact CSL misorientations which may be admitted for the criteria of speciality is also equally important, but has been far from well established. Several contradictory results have been reported on this subject [21,29,30]. For example, Martikainen and Lindroos [29,30] found agreement between the secondary grain boundary dislocation models and the observed periodicity on the boundary in spite of a larger misorientation than that given by the Brandon criterion. This fact indicates the possibility of an accommodating misorientation from certain coincidence orientation relationship to larger secondary rotations than previously assumed.

In the present study, it was found that (1) intergranular chromium carbide was never precipitated on the coherent twin ($\Sigma 3_c$) boundaries, however, needle-like ones were evolved on the incoherent twin ($\Sigma 3_i$) and twin related $\Sigma 9$ boundaries, (2) precipitation was retarded on the low angle grain boundaries ($\Sigma 1$) and well-defined CSL boundaries of $\Sigma 11$ and $\Sigma 15$, (3) on the other hand, carbides were significantly developed on the random high angle grain boundaries. These results were in agreement with previous studies [9,12–14,24,26].

The above results can be understood, in part, in terms of the influence of the grain boundary energy.

The extremely low energy of a coherent twin boundary in a nickel-base alloy [31] could be a reason for the absence of the intergranular carbides on the boundary. Similarly, their suppression on the low angle and CSL boundaries, in comparison with that on the random boundaries, could also be attributed to the difference in their grain boundary energies. It is well known that the grain boundary energy increases in a linear manner as the misorientation increases up to 10–15°, and after this stage the grain boundary energy is almost independent of the misorientation, with the energy cusps at given CSL misorientations [15]. The changes of the grain boundary energy could, therefore, be responsible for the observed intergranular carbide morphology on the various types of grain boundaries.

4. Conclusions

(1) Many annealing twins were present in the thermally treated Alloy 690 due to its low stacking fault energy. The intergranular carbides were significantly developed along most of the grain boundaries. The carbides precipitated on the grain boundaries were identified as Cr-rich $M_{23}C_6$, and found to have a cube–cube orientation relationship such as $\{100\}_{\gamma}\|\{100\}_{M_{23}C_6}$, $\langle 100\rangle_{\gamma}\|\langle 100\rangle_{M_{23}C_6}$ with one grain.

(2) The grain boundaries with coarse and discrete carbides were characterized as random high angle (or general). On the other hand, fine and faceted carbides were densely distributed on the low angle grain boundaries. Carbides were never found on the coherent twin boundaries, however, needle-like ones were evolved on the incoherent and twin related boundaries. On the CSL boundaries established by the Brandon criterion, carbides were rarely precipitated or their morphology was similar to the case of the low angle grain boundaries. Consequently, the precipitation of the intergranular carbides was retarded (or suppressed) on the low angle and CSL boundaries, in comparison with that on the random high angle grain boundaries. The precipitation behavior of the intergranular carbides could be, in part, explained by the influence of the grain boundary energy.

Acknowledgments

This work has been carried out as a part of the Steam Generator Materials Project under the Nuclear R&D Program sponsored by MOST in Korea.

References

[1] T.U. Marston, R.L. Jones, in: Proc. 5th Int. Symposium on Environmental Degradation of Materials in Nuclear Power Systems – Water Reactors, Monterey, CA, 25–29 August 1991, American Nuclear Society, La Grange Park, IL, 1992.
[2] R.A. Page, Corrosion 39 (1983) 409.
[3] S.M. Payne, P. McIntyre, Corrosion 44 (1988) 314.
[4] P.K. De, S.K. Ghosal, Corrosion 37 (1981) 341.
[5] G.P. Airey, Optimization of metallurgical variables to improve corrosion resistance of Inconel Alloy 600, EPRI, NP-3051, 1983.
[6] J.R. Cels, Corrosion 34 (1978) 198.
[7] S.M. Bruemmer, C.H. Henager Jr, Scr. Metall. 20 (1986) 909.
[8] S.M. Bruemmer, L.A. Charlot, C.H. Henager Jr, Corrosion 44 (1988) 782.
[9] M.H. Lewis, B. Hattersley, Acta Metall. 13 (1965) 1159.
[10] L.K. Singhal, J.W. Martin, Trans. Metall. Soc. AIME 242 (1968) 814.
[11] S. Lartigue, L. Priester, Acta Metall. 31 (1983) 1809.
[12] E.A. Trillo, L.E. Murr, J. Mater. Sci. 33 (1998) 1263.
[13] E.A. Trillo, L.E. Murr, Acta Mater. 47 (1999) 235.
[14] H. Liu, M. Gao, D.G. Harlow, R.P. Wei, Scr. Metall. Mater. 32 (1995) 1807.
[15] R.W. Balluffi, Metall. Trans. A 13A (1982) 2069.
[16] D.G. Brandon, Acta Metall. 14 (1966) 1479.
[17] H. Grimmer, W. Bollmann, D.H. Warrington, Acta Crystallogr. A 30 (1974) 197.
[18] D.A. Smith, R.C. Pond, Int. Met. Rev. 21 (1976) 61.
[19] C.T. Young, J.H. Steele Jr, J.L. Lytton, Metall. Trans. 4 (1973) 2081.
[20] G.L. Bleris, J.G. Antonopoulos, Th. Karakostas, P. Delavignette, Phys. Stat. Sol. (a) 67 (1981) 249.
[21] M. Dechamps, F. Baribier, A. Marrouche, Acta Metall. 35 (1987) 101.
[22] ASTM E112-88, Standard Method for Determining Average Grain Size, vol. 03.01, ASTM, Philadelphia, 1992, p. 294.
[23] A.L. Bowman, G.P. Arnold, E.K. Storms, N.G. Nereson, Acta Crystallogr. B 28 (1972) 3102.
[24] Y.B. Lee, J.S. Jang, D.H. Lee, D.Y. Lee, I.H. Kuk, J. Kor. Inst. Met. Mater. 35 (1997) 935.
[25] A. Morawiec, J.A. Szpunar, D.C. Hinz, Acta Metall. Mater. 41 (1993) 2825.
[26] T.M. Angeliu, G.S. Was, Metall. Trans. A 21A (1990) 2097.
[27] G. Gottstein, F. Schwarzer, Mater. Sci. Forum 94–96 (1992) 187.
[28] S. Hirth, G. Gottstein, Acta Metall. 46 (1998) 3975.
[29] H.O. Martikainen, V.K. Lindroos, Acta Metall. 31 (1983) 1909.
[30] H.O. Martikainen, V.K. Lindroos, Acta Metall. 33 (1985) 1223.
[31] L.E. Murr, Interfacial Phenomena in Metals and Alloys, Addison-Wesley, Reading, MA, 1975 p. 138.